INTERNATIONAL JOURNAL OF AUTOMOTIVE AND MECHANICAL ENGINEERING
ISSN: 2229-8649 e-ISSN: 2180-1606
VOLUME 22, ISSUE 2, 2025, 12430 - 12442
DOI: https://doi.org/10.15282/ijame.22.2.2025.14.0951

RESEARCH ARTICLE

Effect of LiDAR Mounting Parameters and Speed on HDL Graph SLAM-Based 3D Mapping for Autonomous Vehicles

Law Jia Seng[1], Muhammad Aizzat Zakaria[1,2,3]*, Maryam Younus[1,2], Ericsson Yong[1,2], Ismayuzri Ishak[1,2,3], Mohamad Heerwan Peeie[2,3,4] and M. Izhar Ishak[2,3,4]

[1]Faculty of Manufacturing and Mechatronic Engineering Technology, Universiti Malaysia Pahang Al-Sultan Abdullah, 26600 Pekan, Pahang, Malaysia
[2]Autonomous Vehicle Laboratory, Centre for Automotive Engineering, Universiti Malaysia Pahang Al-Sultan Abdullah, 26600 Pekan, Pahang, Malaysia
[3]Centre for Advanced Industrial Technology, Universiti Malaysia Pahang Al-Sultan Abdullah, 26600 Pekan, Pahang, Malaysia
[4]Faculty of Mechanical and Automotive Engineering Technology, Universiti Malaysia Pahang Al-Sultan Abdullah, 26600 Pekan, Pahang, Malaysia

ABSTRACT – Generating high-accuracy 3D maps using Light Detection and Ranging (LiDAR) technology remains a critical challenge in autonomous vehicle (AV) development. While 3D mapping is foundational for reliable AV navigation, its accuracy is often compromised by poor LiDAR sensor calibration and external factors such as motion distortion. This study investigates the physical calibration of a LiDAR sensor mounted on a moving vehicle and its effect on 3D map generation using the HDL Graph SLAM algorithm. HDL Graph SLAM was selected as the offline post-processing method due to its self-correcting functions for estimating and auto-correcting positional errors from LiDAR data. Tests were conducted by varying the sensor tilt angle at -5°, 0°, +5°, and +10° and driving speeds at 20 km/h, 30 km/h, and 40 km/h. Results showed that a 0° angle at 30 km/h produced the most accurate 3D map, achieving a Root Mean Square Error (RMSE) of 0.0812 for straight paths and 0.1345 for curved paths. These findings demonstrate the significance of physical mounting parameters and speed on mapping performance. The study provides practical recommendations for LiDAR installation to enhance 3D mapping reliability under real-world road conditions.

ARTICLE HISTORY
Received : 10th Dec. 2024
Revised : 15th Mar. 2025
Accepted : 20th May 2025
Published : 27th June 2025

KEYWORDS
HDL Graph Slam
LiDAR
Odometry
Environmental mapping
HD maps

1. INTRODUCTION

Light Detection and Ranging (LiDAR) technology is a fundamental sensing modality for autonomous vehicle (AV) navigation, particularly in generating high-fidelity three-dimensional (3D) environmental maps. Despite its widespread adoption, the accuracy and robustness of LiDAR-based mapping systems are significantly influenced by sensor calibration and physical deployment parameters. Factors like vehicle speed, sensor orientation, and mounting configuration can introduce noise, motion distortion, and mapping inconsistencies in dynamic environments. While substantial research has focused on algorithmic advancements in simultaneous localization and mapping (SLAM), limited studies have addressed the impact of physical sensor alignment on LiDAR performance. This study fills this gap by comprehensively analyzing how varying tilt angles and driving speeds affect the quality of 3D maps produced using the high-definition LiDAR graph-based simultaneous localization and mapping (HDL Graph SLAM) algorithm (*hdl_graph_slam*). The *hdl_graph_slam* is an open-source Robotic Operating System (ROS) package designed for real-time six degrees-of-freedom (6DOF) SLAM using 3D LiDAR data. It employs a 3D graph-based SLAM framework that incorporates Normal Distributions Transform (NDT) scan matching for odometry estimation and loop closure detection. The system also integrates various graph constraints, including GPS, IMU-derived acceleration (gravity vector), IMU orientation (magnetic sensor), and floor plane detection from the point cloud data. The findings offer empirical insights that can inform practical LiDAR installation strategies for AV perception systems in real-world deployment scenarios.

HDL Graph SLAM algorithm is used to produce 3D maps for road environments. HDL Graph SLAM is an advanced implementation of 3D Graph SLAM using a 3D LiDAR. Graph SLAM is a technique that estimates the robot's trajectory simultaneously and creates a map of the environment. The pattern of the graph represents a network of nodes connected by edges. The 3D LiDAR sensor would produce beams and measure the time to bounce back from objects to create a 3D point cloud. This HDL Graph SLAM method provides considerable advantages in making 3D maps due to multiple error estimation. It will estimate the sensor's position by iteratively matching consecutive LiDAR scans. It also includes loop detection to correct accumulated errors and optimize the pose graph. This method supports constraints such as GPS, IMU Acceleration, IMU Orientation and Floor Plane. Based on the advantages, the HDL Graph SLAM is mostly used for indoor and outdoor scanning and mapping.

The HDL Graph SLAM algorithm creates robust 3D maps when applied in real-world scenarios, instilling a sense of reliability. Practical experiments were conducted to explore its full potential. In this study, a fixed model LiDAR sensor

*CORRESPONDING AUTHOR | M. Aizzat Zakaria | ✉ maizzat@umpsa.edu.my

was integrated with the HDL Graph SLAM method to generate accurate and reliable 3D maps for outdoor environments. Sensor calibration was performed to meet the research objectives. To establish reliable communication with the LiDAR sensor, the Robot Operating System (ROS) Noetic distribution was deployed, further improving mapping robustness. Based on the findings, recommended physical parameters are proposed for mounting a LiDAR sensor on a sedan-type vehicle to ensure 3D mapping reliability in autonomous driving applications. This study is novel in its systematic evaluation of LiDAR sensor mounting angles and vehicular speed variations in a real-world scenario. Unlike prior works that focus predominantly on algorithmic performance, our investigation addresses the physical calibration aspect, which directly impacts the fidelity of HDL Graph SLAM-based 3D mapping in dynamic outdoor environments.

2. RELATED WORK

2.1 Performance of Mapping Algorithms Due to a Change in Moving Speed

Changes in moving speed can significantly impact the performance of 3D mapping algorithms. This is because the speed at which a robot or vehicle moves affects the quality and accuracy of the mapping data collected. There are a few evaluation methods to evaluate the performance of LiDAR according to moving speed, such as Absolute Pose Error (APE), Relative Pose Error (RPE), and Number of Point Clouds (NPCs), as discussed in [1] and [2]. From findings, it claims that changing speeds can introduce skew distortion in accumulated point clouds from a LiDAR, and slower feature detectors in the visual SLAM frontend can lose the tracked landmarks. Also, one of the findings suggests that amplitude and wind speed are not the sole determinants of RMSE and implies that wind direction may also play a significant role [3].

Furthermore, when scanning an object with a relative velocity to the sensor, the object changes the position in the sensor's Field of View (FoV) within one LiDAR frame [4]. To overcome this problem, one of the researchers experimented on the route with speed change to view the performance of different algorithms while changing moving speed. The result showed that the HDL Graph SLAM algorithm has the lowest value of root mean square error due to the loop closure capabilities, which help the estimate's accuracy [2]. These findings highlighted the effect of velocity on LiDAR while the sensor was mounted on moving vehicles. LiDAR is sensitive to many factors, including speed of motion, since the wind comes through the LiDAR sensor. Higher speed would bring efficiency to research in terms of time, but it would also carry the risk of decreasing the accuracy of the reconstructed 3D maps.

2.2 Outdoor and Indoor SLAM

From the findings, the visual SLAM algorithms' performance worsens as the camera moves away from the ground [2]. This indicates that the different positions of the LiDAR sensor mounted on the vehicle would also affect the performance of the SLAM algorithm. Other than that, Akpınar et al. [5] found that the HDL Graph SLAM algorithm gives more accurate results than other algorithms in the staircase environment. However, more precise results are obtained with the A-LOAM and HDL Graph SLAM algorithms than with the LOAM. The findings show that one mapping algorithm does not always perform perfectly in every environment. Recent studies show that increasing the resolution of 3D LiDAR sensors can improve SLAM robustness and reduce mapping error under varying speed conditions [10]. A tightly integrated LiDAR-IMU-wheel encoder SLAM system has shown high accuracy in real-time mapping under varying motion conditions [11]. In dynamic environments, LiDAR-based SLAM systems have also been successfully used to detect and track moving obstacles for safe autonomous navigation [8]. Beyond vehicular contexts, LiDAR-SLAM systems have been extended to complex terrains, such as archaeological sites, to assess rock slope stability using autonomous scanning methods [9]. These findings highlighted the performance difference for each SLAM mapping algorithm for different environments. Different scales of SLAM maps require different types of setups to explore each mapping algorithm's performance fully. Future research should focus on scalability, robustness, and real-time performance to allow for the wide usage of SLAM technology across the autonomous vehicles field.

2.3 Effect of Environmental Conditions

LiDAR sensors are susceptible to various factors that can affect performance since LiDAR is an optical technology that acts as robot perception. LiDAR sensors have proven that it is possible to differentiate different weather types, which shows that the experiment's environmental condition would affect LiDAR sensing ability, providing inaccurate results [6]. The previous research shows that all four weather conditions adversely influence LiDAR detection data [7]. For rain, the detection probability of the LiDAR sensor will start dropping at 10mm/h of rain, and it might lose detection of the target with the onset rain. One of the safety issues for autonomous vehicle driving systems is that they will lose their ability to detect when it rains heavily. The LiDAR would still function in close range to detect the road environment, but it is unsuitable for long paths. For sunlight, LiDAR sensors need to avoid being illuminated directly by sunlight because it will distract the light pulses, signaling between the sensor and the target. This scenario shows that the sunlight will influence the sensor as background radiation or via a direct path from the sun to the sensor. To set up the experiment for 3D mapping, a clear sky is the best weather condition to obtain the most accurate LiDAR data for developing 3D maps. Furthermore, one of the findings indicates that the NPCs were found to decrease on rainy days compared to sunny days, and a rainfall of 40mm/h to 70mm/h caused the data for some materials not to be collected. Recent research has proposed SLAM-based systems specifically designed to maintain high-accuracy mapping under extreme or variable weather conditions, including channels affected by natural hazards [10]. Simulated models have also been developed to replicate

LiDAR signal interference due to rain, fog, or other scattering phenomena, offering physics-based tools to evaluate SLAM robustness in adverse environments [11].

2.4 Sensor Calibration and Mounting Positions

Previous research has concluded that there are challenges to overcome in reducing inaccurate LiDAR data while testing. LiDAR-based SLAM technology must solve issues such as massive computing, scattered coordinate systems, and movement manipulation [8]. The research highlighted the advantages and disadvantages of different LiDAR types and different SLAM types. Then, another research study about autocalibration for LiDAR and Inertial Measurement Unit (IMU) was conducted to mitigate the error of 3D mapping in a structured and dynamic environment. The research emphasized that the correlation between LiDAR sensors and IMU can significantly increase the accuracy of 3D mapping. The experiments show that the auto-calibration method is highly accurate, robust, and repeatable, especially in narrow spaces [9]. The LiDAR sensor and IMU were combined and assembled into a self-assembled backpack, which humans can carry. To further improve the reliability of LiDAR systems, physical parameter calibration for LiDAR sensors on a moving vehicle will be approached in this research to investigate the performance of LiDAR sensors.

To test the performance of the LiDAR sensor under variations in speed and angle, we aim to evaluate its accuracy in generating 3D maps and the impact on Root Mean Square Error (RMSE) metrics. The tests will involve controlled speed variations, with the vehicle moving at 20 km/h, 30 km/h, and 40 km/h, to observe how acceleration and deceleration affect the completeness of map generation and the performance of the HDL Graph SLAM algorithm. Simultaneously, the LiDAR will be mounted at different angles, such as -5 °, 0°, +5°, and +10°, to assess how changes in the field of view and ground-plane detection influence the accuracy of data collection. Data from these tests will be collected using the Robot Operating System (ROS) and processed through the HDL Graph SLAM algorithm for further analysis. The RMSE values will be calculated for both straight and curved paths to identify trends in accuracy based on speed and angle. Variations in speed are expected to influence the quality of point clouds, potentially causing odometry drift errors or skewed data at higher speeds. At the same time, improper angles may hinder ground-plane detection and vertical alignment, impacting the reliability of 3D maps.

Recent advancements have demonstrated that tightly coupled LiDAR-IMU-wheel odometry systems with online calibration can significantly improve real-time mapping accuracy, particularly in structured outdoor environments such as roads and parking areas [12]. Additionally, the mounting positions and orientations of 2D LiDAR sensors have been shown to affect mapping outcomes in structured environments such as orchards, highlighting the importance of physical setup in SLAM performance [13]. Recent developments in LiDAR-based autonomous navigation highlight the increasing need for optimized sensor configurations. For instance, Haris, an advanced autonomous mobile robot developed by Hamad et al. [14], integrates SLAM with automatic license plate recognition (ALPR) for smart parking assistance, demonstrating LiDAR's potential in structured indoor and outdoor scenarios. In another study, Hamad et al. [15] proposed a fusion of stereo vision with SLAM to enhance object depth and size estimation, addressing the perception limitations of LiDAR when encountering non-solid or semi-transparent objects. Furthermore, Khan et al. [16] conducted a detailed review of LiDAR vulnerability in connected and autonomous vehicles (CAVs), presenting a threat model and proposing defensive strategies to mitigate spoofing and sensor attacks. These works emphasize the importance of robust LiDAR integration and processing techniques. However, unlike our study, they do not address the practical implications of physical LiDAR calibration, such as sensor tilt and mounting orientation, on mapping accuracy during vehicle motion, which remains a critical gap in field deployment of AV systems.

Moreover, Yong and Zakaria et al. explored 3D LiDAR-based vehicle perception and classification using 3D machine learning algorithms [17]. Their study emphasizes how the structure and orientation of LiDAR point clouds significantly affect object detection and classification accuracy. Although their focus was on deep learning-based perception, the study implicitly highlights the importance of sensor placement and mounting angle, as these factors directly influence the density and distribution of LiDAR point data. Our work builds on this by explicitly investigating the physical calibration and positioning of LiDAR sensors to improve the reliability of 3D mapping in autonomous driving environments. Also, reliable LiDAR point data can be used for the development of the LiDAR edge-based planning algorithms [18].

In summary, while prior research has advanced the development of SLAM algorithms and their applications in both indoor and outdoor environments, there remains a significant gap in understanding how the physical mounting parameters of LiDAR sensors affect 3D mapping quality in real-world autonomous driving scenarios. Most existing studies emphasize software improvements or sensor fusion yet overlook the influence of basic physical configurations, such as sensor tilt angle and vehicle speed, on LiDAR data fidelity. In contrast, this study provides a comprehensive experimental evaluation of HDL Graph SLAM performance by systematically altering LiDAR sensor inclination and vehicle speeds under outdoor conditions. The results highlight how different configurations impact RMSE in both straight and curved trajectories, offering practical design insights for sensor integration in autonomous vehicle platforms. This contribution is expected to assist practitioners, engineers, and researchers in developing more reliable and precise LiDAR-based mapping frameworks for AVs.

3. METHODOLOGY

3.1 Robot Operating System

Robot Operating System (ROS) is an open-source software framework for robotics development that provides a flexible and distributed platform for building robotic systems. It enables developers to create and share code across different robots and platforms easily, supports a wide range of hardware, and includes tools for debugging and visualizing robotic systems. Among various versions of ROS, ROS Noetic was chosen as a tool for 3D mapping throughout this research. Although ROS 1 will end service by 2025, its vast community has provided many resources since ROS 1 has existed for a long time. Furthermore, the author tested and used the HDL Graph SLAM algorithm in ROS Melody and Noetic, which performed well in running the mapping algorithm. ROS Noetic provides built-in tools such as Rviz for real-time simulation while reconstructing LiDAR maps.

3.2 HDL Graph SLAM

HDL Graph SLAM is an open-source Robot Operating System (ROS) package for real-time 6 Degree of Freedom SLAM using a 3D LiDAR. This package is one of the packages to use for 3D mapping. Multiple point clouds are used to create a map in a 3D visualization tool in ROS with the combination of loop detection, odometry estimation, and NDT scan matching. It supports several graph constraints, including GPS, floor plane detection, IMU acceleration, and IMU orientation.

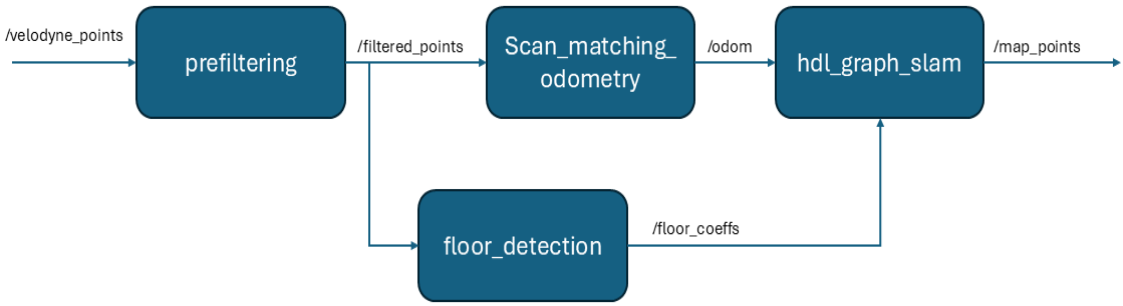

Figure 1. Nodes of the HDL Graph SLAM Algorithm

The algorithm's builder proposed loop-closing and plane-based constraints to create map correction constraints [19] semi-automatically. Then, the plane constraint parameter should be applied to correct the accumulated rotational error in getting the completely flat resultant map to avoid obtaining inaccurate mapping results [20]. The HDL Graph SLAM has become one of the most popular choices for reconstructing 3D maps throughout the research due to its loop-closing algorithm, sensor position optimization, and robustness. The progress of generating HDL map points contains four notelets: prefiltering, scan_matching_odometry, floor detection, and *hdl_graph_slam* as in Figure 1. Cloud points received by the LiDAR sensor will be filtered and processed through all the notelets and produced/map points to generate a 3D map in RViz.

3.3 Experimental Setup

The LiDAR sensor used in this research is Robosense C16 (16-channel), as shown in Figure 2, and its specifications are in Table 1. It has a 360-degree field of view, allowing full coverage in outdoor scanning. The LiDAR sensor used in this research is mechanical. A mechanical LiDAR is the oldest type of LiDAR sensor and continuously spins a mirror to scan the environment. This sensor measures the distance and shape of objects surrounding using the Time-of-Flight Distance Measurement method, which measures the time needed for an emitted laser pulse to reflect into the LiDAR sensor. The properties of the LiDAR sensor chosen can provide a significant advantage in large-scale mapping applications related to this research.

The metal frame consisted of 4 suction cups as the base so that the frame could be attached and stabilized on the top of the moving robot. For this research, the test car uses the Proton Persona with the dimensions of 4366 mm x 1722 mm x 1564 mm. The LiDAR sensor was mounted on the test car with the fixed parameters of 175 cm height, 63 cm to the side and 212 cm from behind. Next, one of the car's windows will be lowered according to the placement of a personal laptop. To power up the LiDAR sensor, a 12V battery was prepared and placed on the vehicle's backseat to supply sufficient electricity for the LiDAR sensor. Next, a LAN cable will be connected between the personal laptop and the interface box of the LiDAR sensor to transmit the data received by the sensor. To check the connectivity of LiDAR to personal laptops, the light indicator on the interface box lights up red and green to show sufficient power input and output. In Ubuntu, the LiDAR driver package is run to check the present working condition and avoid hardware malfunction.

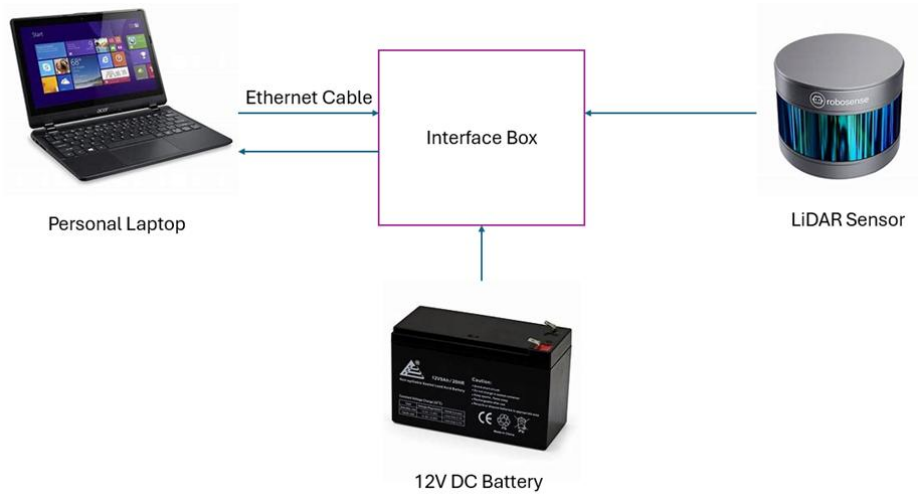

Figure 2. Illustration for the connection of a LiDAR sensor with a personal laptop

Table 1. Specification of the Robosense C16 (16-channel)

Features	Specifications
Method of Measurement	Time of Flight Distance Measurement
Channel	16 Channels
Measurement Range	40 cm to 150 m (on 20% reflectivity target)[2]
Accuracy	±2 cm (typical)[3]
Field of View (Vertical)	$\pm 15.0^{o}$ (30^{o} in total)
Angular Resolution	2^{o}
Field of View (Horizontal)	360^{o}
Angular Resolution (Horizontal/Azimuth)	0.1^{o}(5 Hz)to 0.4^{o} (20 Hz)
Rotation Rate	300/600/1200 rpm (5/10/20 Hz)

Figure 3. Installation of LiDAR sensor with metal frame on the top of the test car

3.4 Angle Inclination

The LiDAR sensor was mounted on a metal frame (Figure 3), and its center of rotation was based on the handle of the metal frame. The trigonometry method (Figure 4) was applied to change the angle of the LiDAR sensor to achieve its inclination.

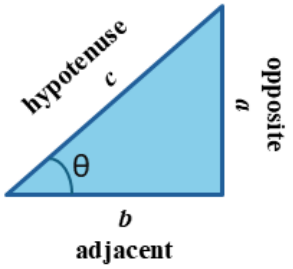

Figure 4. Trigonometry Triangle

A level ruler and a steel tape ruler were used to determine the horizontal level of the LiDAR sensor and measure its length. Before that, a meter ruler was placed above the LiDAR sensor to identify the horizontal level (0◦ degrees) as the starting angle for the test.

$$tan\ (\theta) = \frac{Opposite}{Adjacent} \tag{1}$$

By substituting the value Adjacent to the rotation center from the metal frame to the LiDAR sensor and the value of angle to test angle, the height value from the surface to the LiDAR sensor can be determined in degrees. For the direction of inclination, the negative value will indicate that the inclination angle is facing upward, and the positive value will indicate that the angle will face toward the plane level.

3.5 Mapping Progress

Figure 5 shows the mapping process of the HDL SLAM algorithms. It starts with the reading from 3D LiDAR sensors and is published as /rslidar_points topic in point cloud message format types. The topic is then subscribed by a subscribing node and a hdl_slam_graph node that processes the SLAM algorithm to generate a 3D map. After the mapping process finishes, the map will be saved using a service called /hdl_slam_graph/save the map. The algorithms then publish the odometry output of the rotation and position.

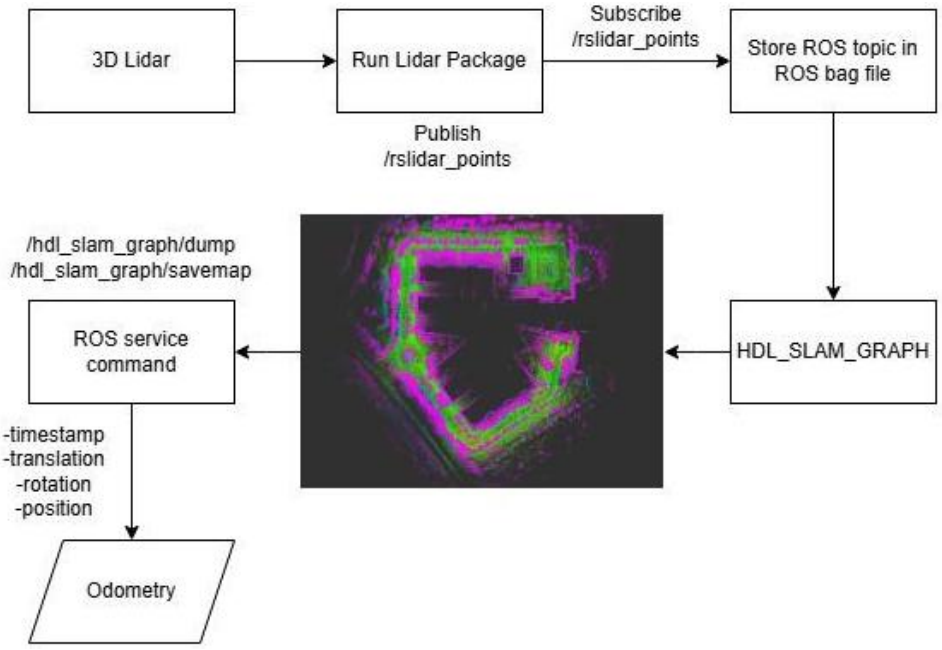

Figure 5. HDL_SLAM_GRAPH 3D Mapping Workflow

The data is collected in ROS bag files using the Robot Operating System (ROS) environment in a personal laptop built with a GTX1650 GPU and an Intel(R) Core (TM) i7-9750H CPU @ 2.60GHz. The data from the LiDAR sensor was recorded in the form of a ROS topic inside a bag file. The ROS bag replayed the live data stream from the LiDAR sensor while running the HDL SLAM algorithm. The SLAM algorithm will be run in Ubuntu Linux before replaying the ROS bag. The 3D visualization tool Rviz needs to be launched to visualize the outcome of the data collection. Hence, start running the ROS bag while running the SLAM algorithm and Rviz to allow the ROS topic to be published into the SLAM algorithm and shown on Rviz to view the 3D maps. Lastly, necessary information, such as odometry, can be saved by using the ROS service command.

3.6 Error Metrics (Root Mean Square Error)

To determine the accuracy of the generated 3D mapping, the technique of Root Mean Square Error (RMSE) will be applied to this research as in Equation 2 to Equation 4. The root mean square error will be used in mathematics to calculate the difference between actual observed values and values predicted by machine algorithms. In this research, the evaluation method for evaluating the accuracy of the 3D map used the LiDAR 2D trajectory in the x and y axes to compare with the reference path. The RMSE formula will be a 2D formula for the x-axis and y-axis instead of a 3D one. According to the statement of RMSE, the lower the value of RMSE, the smaller the difference between the predicted value and the actual value, which also indicates that the model or algorithm is performing well.

$$RMSE_x = \sqrt{\frac{1}{n}\sum_{i=1}^{n}\left(\hat{x}_{pred} - x_{actual}\right)^2} \tag{2}$$

$$RMSE_y = \sqrt{\frac{1}{n}\sum_{i=1}^{n}\left(\hat{y}_{pred} - y_{actual}\right)^2} \tag{3}$$

$$RMSE_{TOTAL} = \sqrt{RMSE_x^2 + RMSE_y^2} \tag{4}$$

$\hat{x}_{pred}$: Data predicted/estimated in x-axis
x_{actual} : Actual/Reference data in x-axis
$\hat{y}_{pred}$: Data predicted/estimated in y-axis
y_{actual} : Actual/Reference data in y-axis
n : Number of data points

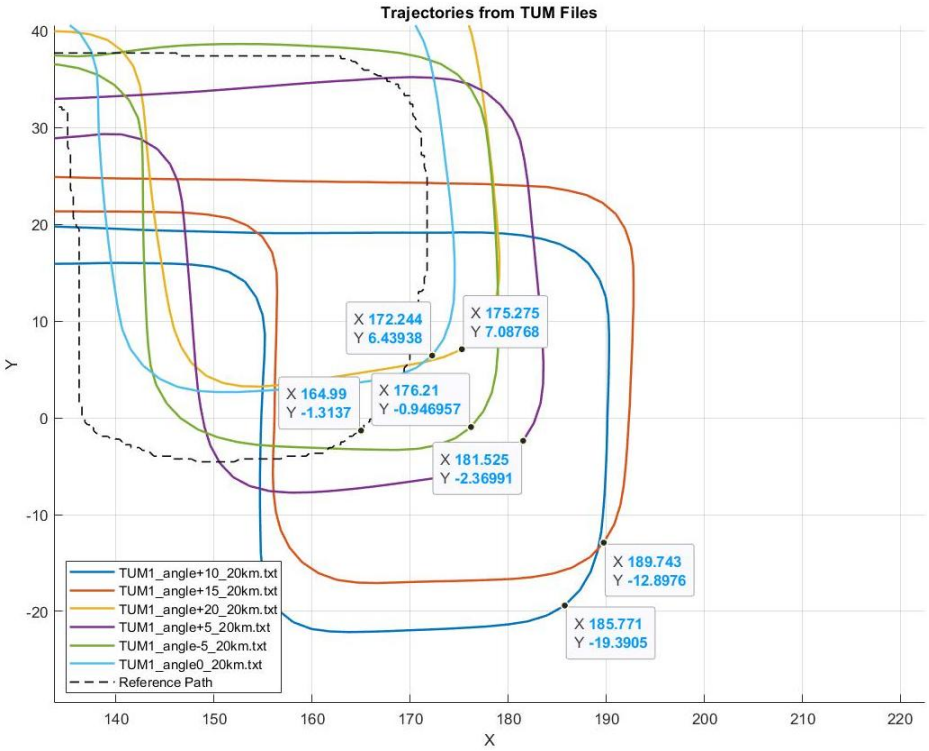

Figure 6. Seven selected points from MATLAB graph for each trajectory along the curved path

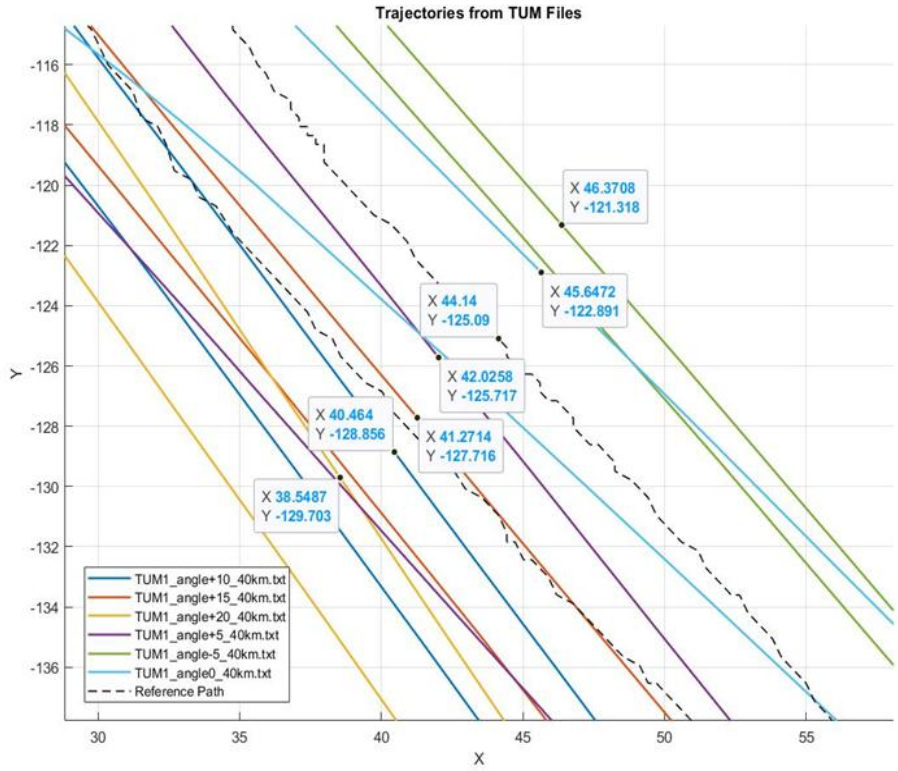

Figure 7. Seven selected points from the MATLAB graph for each trajectory along a straight path

Using MATLAB, the 2D trajectory will be plotted together with the reference path in the exact figure. From Figures 6 and 7, seven points were selected and extracted from different trajectories to calculate the root mean square error for the curving and straight paths. Since the test environment contained multiple junctions of curving and straight paths, two types of root mean square error were determined for both types of roads to view the performance of LiDAR at different road conditions.

3.7 Route of Accelerating and Decelerating

Figure 8 shows the path of changing the speed of the test vehicle while moving on the faculty. To evaluate the performance of the LiDAR sensor at different speeds, the vehicle's speed was increased to a specific velocity, and that speed was maintained while collecting the data. The green color of the path indicates the acceleration of the moving car to a particular speed. The speed range in the green color path is controlled from 20km/h to 40km/h. The red color of the path indicates the deceleration of the moving car to a low speed while facing a sharp turn in a limited space area. The speed range of the red color path would range between 10km/h and 20km/h.

Figure 8. Route of accelerating and decelerating

4. EXPERIMENTAL RESULTS

4.1 Data Preparation

During offline environmental mapping, not all recorded data can generate complete 3D maps in RViz. As shown in Table 2, the results of 3D map generation are categorized into three different groups. The green color indicates that the full 3D map was generated successfully without any errors. The yellow color indicates that although the process of reconstructing a complete 3D map encountered loop closure failure during mapping, the algorithm was able to correct it through pose optimization. The blue color shows that the 3D map generation was undertaken successfully, but under the consequences of the poor performance of HDL Graph SLAM. The time taken for reconstructing 3D maps needs to be improved significantly, including reducing errors during the process. The red color indicates the failure of 3D map generation due to heavy odometry drift error. From observation, the maps of LiDAR angle below -5 cannot be reconstructed correctly in RViz, and these results were not suitable for further analysis. These consequences were due to the Lidar sensor not being able to detect the ground plane for the environment, causing continuous z-direction odometry shift and tilting of the map. This error causes a mapping error and then tilts the map upward to generate the wrong pattern of 3D maps. The data for angles -10, -15 and -20 were excluded from the metric analysis to increase the integrity of the results, as the LiDAR sensor is oriented upwards.

Table 2. Results of Generating 3D Maps (Green: Complete map without errors; Yellow: Loop closure corrected; Blue: Map generated with degraded performance; Red: Mapping failed due to odometry drift)

Speed Lidar Angle (degree)	3D Maps					
	First Recording			Second Recording		
	20km/h	30km/h	40km/h	20km/h	30km/h	40km/h
-20						
-15						
-10						
-5						
0						
5						
10						
15						
20						

4.2 3D Maps Generation

Using the HDL SLAM Graph algorithm, 3D maps for different angles of the Lidar sensor were reconstructed in the visualization tools, as shown in Figure 9. The details of the maps, such as odometry, timestamp, translation, rotation, and rotation, were used to reconstruct 3D maps for different angles of the Lidar sensor using the HDL SLAM Graph algorithm, as shown in Figure 9. The details of the maps, such as odometry, timestamp, translation, rotation, and point cloud information, were extracted from the map to prepare for further analysis.

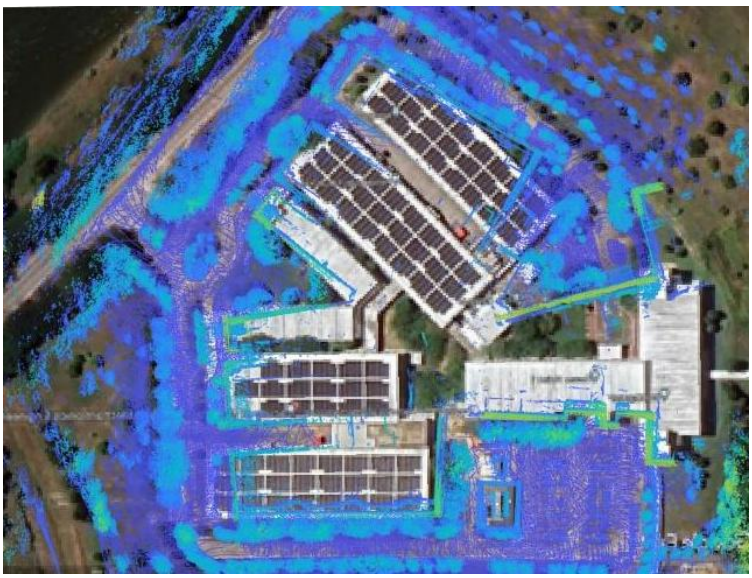

Figure 9. Overlapping 3D LiDAR map on the Faculty UMPSA

4.3 Ground Truth/Reference Trajectory with Alignment

The information on odometry was extracted from 3D maps and imported into MATLAB to plot the graph in 2D dimensions using x and y coordinates. This method is similar to the graph-generation method to predict the road network graphs from aerial images [21]. Then, the eagle view of the Faculty of Manufacturing and Mechatronic Engineering Technology in UMPSA was captured and saved using Google Earth Pro. The image was imported into MATLAB and displayed as the background of a graph with the same scale as the LiDAR trajectory data. The reference path is black, while the trajectory of the odometry outputs is shown in Figure 10. The RMSE is computed to calculate the trajectory odometry to the reference path.

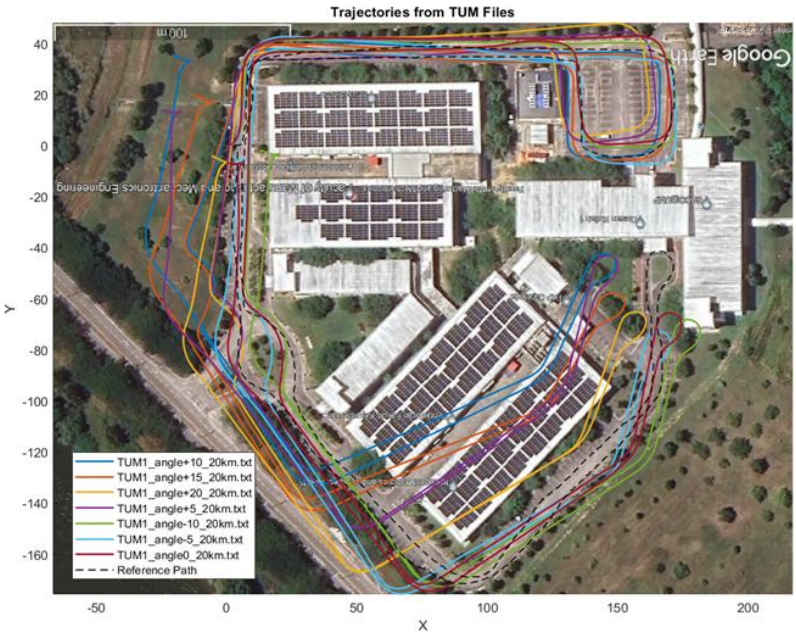

Figure 10. Overlay of LiDAR and Reference Trajectory of the faculty image

4.4 RMSE for the Straight Path

From Table 3, Angles 0, +5, +10 and +15 have higher error values than Angles -5 and +20. Then, there is a trend of decreasing error value while the test car's moving speed increases. This is because the motion compensation in the Robosense LiDAR channel 16 will automatically help to improve the accuracy of LiDAR at high speeds. Table 3 shows the average value of RMSE for the Curve Path of Angle -5 to Angle +20, which is visualized in Figure 11. However, overall, Angle-5 degrees had the lowest root mean square error value among the test data, as shown in Figure 11.

Table 3. Average Value of RMSE for Straight Path of Angle -5 to Angle +20 degrees

Speed	Angle (degree)					
	-5	0	5	10	15	20
20km/h	9.501650	18.32847	12.77858	29.89546	22.83834	14.85870
30km/h	7.583268	25.33391	29.94313	33.27483	24.61398	14.89875
40km/h	3.182261	17.01607	15.48938	19.16677	16.17628	13.27444

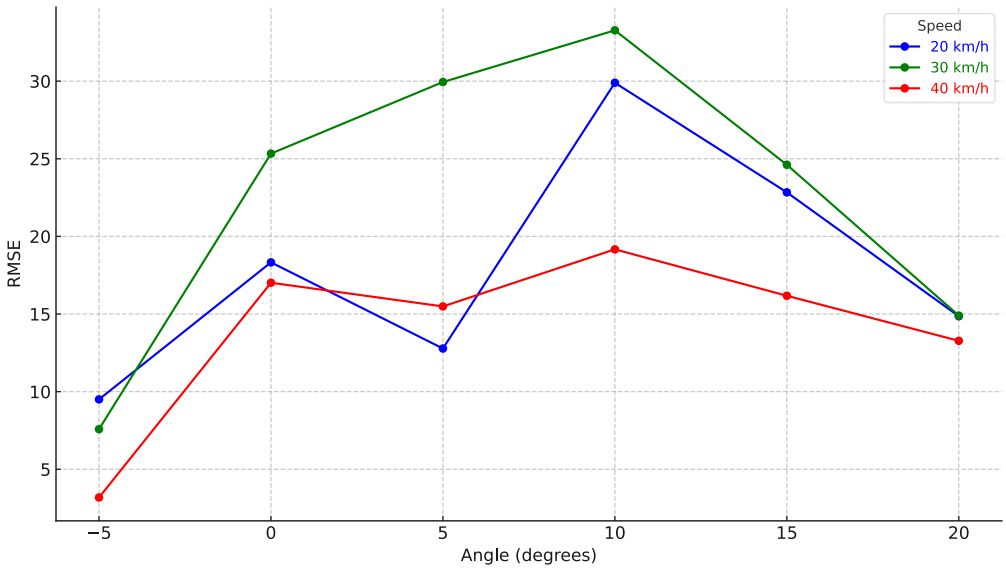

Figure 11. Graph of RMSE against LiDAR angle for straight path

4.5 RMSE for Curve Path

Table 4 shows the average root mean square error value for the curve path from angle -5 to angle +20, which is visualized in Figure 12, and by looking into only one speed, angles +10, +5 and +15 had the lowest Root mean square error value at different moving speeds. Then, from the table above, we can observe that while the test car's moving speed increases, the error value also increases, which means that the accuracy of LiDAR mapping would decrease as well due to the rise in error while driving in a curved path. Furthermore, the scalability of angle-5 was the lowest compared to the other angles. Although an angle of 5 degrees does not have the lowest value of root mean square error, it provides high stability towards LiDAR mapping, which is one of the most crucial keys for high-accuracy map development.

Figure 12 visualizes the root mean square error value for different angles and speeds. Angles +5, +10, and +20 had a huge spike that caused the error to increase significantly while the test car moved in a curved path. Angles -5 and 0 have a few higher values than other angles, but have similar stability to prevent a spike signal.

Table 4. Average Value of RMSE for Curve Path of Angle -5 to Angle +20

Speed	Angle					
	-5	0	+5	+10	+15	+20
20km/h	6.756042	6.131161	3.867921	2.665996	5.922347	7.141040
30km/h	7.394502	7.083348	4.397015	5.106992	7.568335	6.899169
40km/h	7.623731	7.595246	10.372080	7.591344	4.630411	14.535630

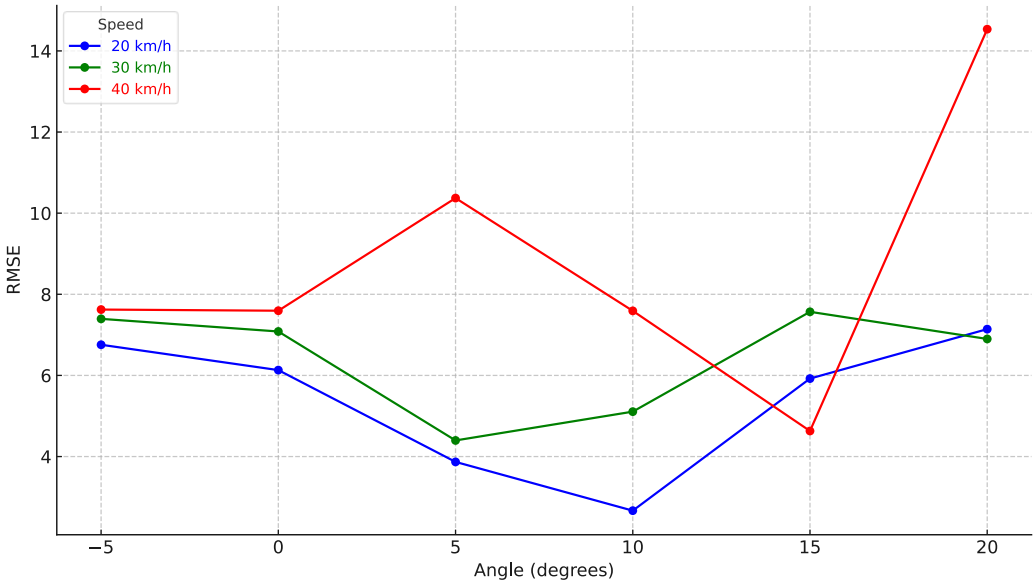

Figure 12. Graph of RMSE against LiDAR angle for curve path

5. CONCLUSIONS

From the results, the most suitable angle for mounting the LiDAR sensor on the top of a Sedan model vehicle is Angle -5. It provides the lowest scalability on root mean square error with 6.756042 at 20km/h, 7.394502 at 30km/h and 7.623731 at 40 km/h in the curve path. Also, this angle had the lowest root mean square error value with 9.50165 at 20km/h, 7.583268 at 30km/h and 3.182261 at 40 km/h in a straight path. The hypothesis is that the higher the speed of the test car, the lower the root mean square error for the HDL Graph SLAM algorithm by using Robosense 16-channel LiDAR, but the risk of having a spike during data collection is a challenge. The speed of the test car was limited to 20 kms/h, 30km/h and 40km/h due to the small spacing of the route. Next, the LiDAR angle was adjustable, but the other parameter, such as the distance of LiDAR from the vehicle sides, was fixed, and this might limit the observation of the performance of LiDAR. To see the mapping results, IMU and GPS can be applied to achieve greater accuracy of 3D maps. The HDL Graph SLAM performance on another model of the test car, such as an SUV, can be tested to view the performance. Then, the mapping environment can change to big and open spaces without limiting the maximum speed change for the test car to view the performance of HDL Graph SLAM. Future research can explore alternative LiDAR sensor models and integrate GPS/IMU modules to enhance 3D mapping accuracy. Future research can explore alternative LiDAR sensor models and integrate GPS/IMU modules to enhance 3D mapping accuracy.

6. FUTURE WORKS

The current study employed HDL Graph SLAM, a 3D LiDAR-based SLAM algorithm developed by Koide et al., which utilizes Normal Distributions Transform (NDT) for scan matching and graph-based optimization for loop closure. While HDL Graph SLAM offers robust mapping capabilities, future work will consider transitioning to more advanced frameworks from the same research group. A recent development by Koide et al. is the GLIM (GPU-accelerated LiDAR-Inertial Mapping) framework [22] – [25], which significantly enhances real-time SLAM performance. GLIM integrates LiDAR and IMU data through a fixed-lag smoother and GPU-accelerated keyframe-based scan matching, improving computational efficiency and mapping accuracy. Unlike HDL Graph SLAM, GLIM supports global trajectory optimization by directly minimizing submap registration errors and can handle multi-sensor fusion, including optional visual inputs. These enhancements make GLIM a promising candidate for deployment in large-scale and complex environments, such as autonomous driving scenarios, where mapping reliability and speed are critical.

ACKNOWLEDGEMENTS

The authors would like to thank the Ministry of Higher Education for providing financial support under the Fundamental Research Grant Scheme (FRGS) No. FRGS/1/2021/TK02/UMP/02/2 (University Reference RDU210103). The authors would like to extend their thanks to the project, ID number PDU243204, and Universiti Malaysia Pahang Al-Sultan Abdullah for laboratory facilities as well as additional financial support under special project grant SPU230101 and internal research grant CDU240136. The authors would also like to thank Cybersecurity Malaysia for the Proton X50 Test Vehicle facility.

CONFLICT OF INTEREST

The authors declare no conflicts of interest as the research was conducted in Universiti Malaysia Pahang, Al-Sultan Abdullah, without the involvement of any third party.

AUTHORS CONTRIBUTION

Law Jia Seng (Data curation; Methodology; Writing- original draft)

Muhammad Aizzat Zakaria (Conceptualization; Supervision; Funding acquisition; Formal Analysis, Writing)

Maryam Younus (Visualization; Writing-review and editing)

Erricson Yong (Data curation)

Ismayuzri Ishak (Investigation)

Mohamad Heerwan Peeie (Writing-review and editing)

M. Izhar Ishak (Writing-review and editing)

REFERENCES

[1] J. Kim, B. J. Park, C. G. Roh, and Y. Kim, "Performance of mobile LiDAR in real road driving conditions," *Sensors*, vol. 21, no. 22, p. 7461, 2021.

[2] C. B. Garigipati, "Evaluation of simultaneous localization and mapping (SLAM) algorithms," M.Sc. thesis, Tampere Univ., Finland, 2021.

[3] M. Thiébaut, L. Furgerot, M. Deroo, L. Guillou, D. El Khamlichi, and M. Le Boulluec, "Experimental evaluation of the motion-induced effects for turbulent fluctuations measurement on floating LiDAR systems," *Remote Sensing*, vol. 16, no. 8, p. 1337, 2024.

[4] L. Haas, E. Urbina, H. Masuda, M. A. de Oliveira, and S. Oh, "Velocity estimation from LiDAR sensors motion distortion effect," *Sensors*, vol. 23, no. 23, p. 9426, 2023.

[5] B. Akpınar, "Performance of different SLAM algorithms for indoor and outdoor mapping applications," *Applied System Innovation*, vol. 4, no. 4, p. 101, 2021.

[6] J. Jorge, T. Barros, C. Premebida, M. Aleksandrov, D. Goehring, and U. J. Nunes, "Impact of 3D LiDAR resolution in graph-based SLAM approaches: A comparative study," in *2024 7th Iberian Robotics Conference (ROBOT)*, 2024, pp. 1–6.

[7] D. Hong, W. Zhao, Q. Shen, Z. Zhou, and C. Du, "A high-precision SLAM system based on LiDAR, IMU and wheel encoders," in *Proceedings of the 5th International Conference on Robotics, Intelligent Control and Artificial Intelligence (RICAI)*, 2023, pp. 905–910.

[8] A. Saha and B. C. Dhara, "3D LiDAR-based obstacle detection and tracking for autonomous navigation in dynamic environments," *International Journal of Intelligent Robotics and Applications*, vol. 8, no. 1, pp. 39–60, 2024.

[9] L. Beltramone, V. De Lucia, A. Ermini, M. Innocenti, D. Silvestri, A. Rindinella, *et al.*, "Applying SLAM-based LiDAR and UAS technologies to evaluate the rock slope stability of the Grotta Paglicci Paleolithic site (Italy)," *GeoHazards*, vol. 5, no. 2, pp. 457–484, 2024.

[10] T. Wang, F. Lu, J. Qin, T. Huang, H. Kong, and P. Shen, "AscDAMs: Advanced SLAM-based channel detection and mapping system," *Natural Hazards and Earth System Sciences*, vol. 24, no. 9, pp. 3075–3094, 2024.

[11] V. Kilic, D. Hegde, A. B. Cooper, V. M. Patel, M. Foster, et al., "LiDAR light scattering augmentation (LiSA): Physics-based simulation of adverse weather conditions for 3D object detection," in *Proceedings of the IEEE International Conference on Acoustics, Speech and Signal Processing (ICASSP)*, 2025, pp. 1–5.

[12] T. Okawara, K. Koide, S. Oishi, M. Yokozuka, A. Banno, K. Uno, et al., "Tightly-coupled LiDAR-IMU-wheel odometry with online calibration of a kinematic model for skid-steering robots," *IEEE Access*, vol. 12, pp. 134728–134738, 2024.

[13] Q. Li and H. Zhu, "Performance evaluation of 2D LiDAR SLAM algorithms in simulated orchard environments," *Computers and Electronics in Agriculture*, vol. 221, p. 108994, 2024.

[14] L. Hamad, M. A. Khan, H. Menouar, F. Filali, and A. Mohamed, "Haris: An advanced autonomous mobile robot for smart parking assistance," in *Proc. IEEE Int. Conf. Consumer Electronics (ICCE)*, 2024, pp. 1–6.

[15] L. Hamad, M. A. Khan, and A. Mohamed, "Object depth and size estimation using stereo-vision and integration with SLAM," *IEEE Sensors Letters*, vol. 8, no. 4, pp. 1–4, 2024.

[16] M. A. Khan, H. Menouar, M. Abdallah, and A. Abu-Dayya, "LiDAR in connected and autonomous vehicles – perception, threat model, and defense," *IEEE Transactions on Intelligent Vehicles*, pp. 1–14, 2024.

[17] E. Yong, M. A. Zakaria, M. H. Peeie, and M. I. Ishak, "3D LiDAR vehicle perception and classification using 3D machine learning algorithm," in *Intelligent Manufacturing and Mechatronics. iM3F 2023*, Lecture Notes in Networks and Systems, vol. 850, Singapore: Springer, 2024, pp. 291–302.

[18] A. Vinayak, M. A. Zakaria, K. Baarath, et al., "A novel triangular-based estimation technique for Bezier curve control points generation on autonomous vehicle path planning at the roundabout intersection," *Journal of Intelligent & Robotic Systems*, vol. 109, p. 89, 2023.

[19] K. Koide, J. Miura, and E. Menegatti, "A portable three-dimensional LiDAR-based system for long-term and wide-area people behavior measurement," *International Journal of Advanced Robotic Systems*, vol. 16, no. 2, p. 9841532, 2019.

[20] K. Koide, J. Miura, M. Yokozuka, S. Oishi, and A. Banno, "Interactive 3D graph SLAM for map correction," *IEEE Robotics and Automation Letters*, vol. 6, no. 1, pp. 40–47, 2021.

[21] Z. Bao, S. Hossain, H. Lang, and X. Lin, "A review of high-definition map creation methods for autonomous driving," *Engineering Applications of Artificial Intelligence*, vol. 122, p. 106125, 2023.

[22] K. Koide, M. Yokozuka, S. Oishi, and A. Banno, "GLIM: 3D range-inertial localization and mapping with GPU-accelerated scan matching factors," *Robotics and Autonomous Systems*, vol. 179, p. 104750, 2024.

[23] K. Koide, "glim: 3D range-inertial localization and mapping," *GitHub Repository*, 2024. [Online]. Available: https://github.com/koide3/glim

[24] K. Koide, "GLIM: 3D range-inertial localization and mapping," *Koide3 Research Projects*, 2024. [Online]. Available: https://koide3.github.io/glim/

[25] J. Jorge, T. Barros, C. Premebida, M. Aleksandrov, D. Goehring, and U. J. Nunes, "Impact of 3D LiDAR resolution in graph-based SLAM approaches: A comparative study," in *Proceedings of the 2024 7th Iberian Robotics Conference (ROBOT)*, Madrid, Spain, 2024, pp. 1–6.